

# Detection of static eccentricity for permanent magnet synchronous motors using the coherence analysis

Mehmet AKAR<sup>1</sup>, Sezai TAŞKIN<sup>2</sup>, Serhat ŞEKER<sup>3</sup>, İlyas ÇANKAYA<sup>4</sup>

<sup>1</sup>*Department of Mechatronics Engineering, Gaziosmanpaşa University, Tokat-TURKEY*

*e-mail: mehmetakar@gop.edu.tr*

<sup>2</sup>*Department of Electronics and Automation, Celal Bayar University, Turgutlu, Manisa-TURKEY*

*e-mail: sezai.taskin@bayar.edu.tr*

<sup>3</sup>*Department of Electrical Engineering, İstanbul Technical University, İstanbul-TURKEY*

*e-mail: seker@elk.itu.edu.tr*

<sup>4</sup>*Department of Electronics and Computer Education, Sakarya University, Sakarya-TURKEY*

*e-mail: icankaya@sakarya.edu.tr*

## Abstract

*This paper reports on work to detect the static eccentricity faults for permanent magnet synchronous motor (PMSM) using spectral analysis methods. Measurements are carried out by collecting the stator current and voltage, torque and speed for healthy and faulty cases of the motor. Static eccentricity case is formed by changing the rotor position in the manner of sliding the shaft on a horizontal axis. As a result of the spectral analysis for the motor currents, side band effects appeared at around the fundamental frequency are determined as a most important indicator of the eccentricity. In addition to this determination, the eccentricity problem is observed from the torque and rotor speed data comparing with each others as well as current and voltage variations.*

**Key Words:** *Permanent Magnet Synchronous Motor, Eccentricity, Fault Diagnosis, Spectral Analysis*

## 1. Introduction

Many mechanical failures in electromechanical machines are related to their bearings. The origin of bearing-centered failures include vibration, misalignment and shaft distortion. Also other faults related rotor problems appear with cracked or broken rotor bars, broken end rings, demagnetized rotor magnets or broken rotor magnets [1].

The early detection of anomalies in the electrical or mechanical parts of electric motors is important to the safe and economic operation of an industrial process. Early fault detection techniques, which are defined for these motors, can significantly reduce the maintenance costs. Thus, condition monitoring studies are proposed for fault diagnosis in electric motors, among which spectral analysis is accepted as one of the outstanding techniques in the literature [2-7].

PMSMs are increasingly used in many commercial and industrial applications because of their high power density, wide constant-power speed range, excellent efficiency, high air-gap flux density and high torque to inertia ratio [8]. The PMSMs are most convenient components for the applications of packaging, glass wood, robotics, handling, etc.

Although is much research on eccentricity faults in induction motors, there are few studies on the PMSM eccentricity fault. Rosero et al. reported an experimental study for diagnosis of broken bearings and eccentricity faults [9]. In this study, stator current harmonics were obtained using via the current spectrum. In another study, they used two dimensional Finite Element Analysis methods for the diagnosis of dynamic eccentricity (DE) [1]. Ebrahimi et al. used the amplitudes of the harmonic components, called an index [10]. The Index was used for noninvasive diagnosis of static eccentricity (SE) in PMSM. Roux et al. studied SE, DE and broken magnet faults using a low power PMSM stator current and voltage [11]. Akar et al. studied on diagnosis of eccentricity fault in PMSM. Motor stator current and voltage harmonics investigated by using LabVIEW Signal Express Toolbox program for healthy and faulty conditions [12].

This work focused on the detection of static eccentricity fault for a PMSM. For this purpose, static eccentricity case is formed by changing the rotor position in the manner of sliding the shaft on horizontal axis. Hence, the data is acquired by means of the torque meter to observe the mechanical changes. Also, electrical quantities like motor current and voltage are taken by the PMSMs driver system as well as speed measurement. This experimental study is repeated for 0% (no-load) and 25% load conditions. In terms of the data analysis procedure, Auto and Cross Power Spectral Density techniques are applied to these data to extract of the related features. As a result, the eccentricity frequencies are determined in the spectral domain. In the literature, although the most popular approach is motor current signature analysis, in this study, speed and torque measurements are also considered as well as the motor current signals.

## 2. Fault classification in electric machinery and eccentricity problem

Faults in motors disturb their operation and shorten their useful life. As such, prediction, diagnosis and detection of faults is very important to maintain their service.

The eccentricity fault of a stator and rotor is due mainly to mechanical reasons. In this fault, symmetrical axis of stator, symmetrical axis of rotor and rotation axis of rotor are displaced to each others. This displacement of symmetrical axes can be classified into static, dynamic and mixed eccentricities. Of static eccentricity, the rotor rotation axes coincide with its symmetrical axes, but displaced with respect to the stator symmetrical axes. In such a case, the air gap distribution around rotor lacks uniformity but is time-independent [1].

Many faults can occur in electrical machines. Table 1 lists those faults and the fraction with which they occur. [13].

Nearly 40–50% of all motor failures are related to mechanical faults [8]. Mechanical faults have caused to a noise and vibrations due to unbalanced magnetic pull. These faults can be diagnosed by monitoring electrical quantities (motor current, voltage and instantaneous power) and mechanical quantities (vibrations and torque oscillations) [14]. In order to detect these faults, a number of diagnostic methods are employed [15]:

- Electromagnetic field monitoring;
- Noise and vibration monitoring;

- Acoustic noise measurements;
- Motor-current signature analysis (MCSA).

**Table 1.** Distribution in the types of motor failures.

Faults	IEEE-IAS (%)	EPRI (%)
	Electrical Safety Workshop	Electric Power Research Institute
Bearing	44	41
Winding	26	36
Rotor	8	9
Other	22	14

In a healthy motor, the rotor is center-aligned with the stator bore, and the rotor’s center of rotation is the same as the geometric center of the stator bore, as illustrated in Figure 1 [16].

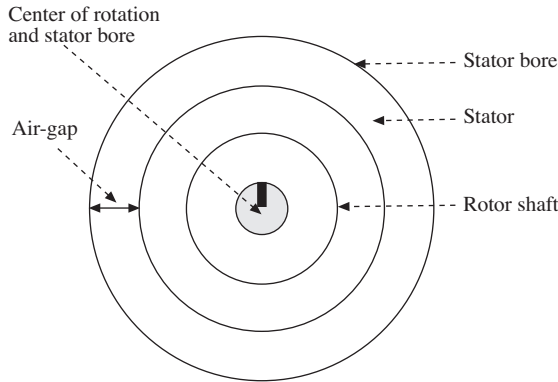


**Figure 1.** Healthy motor.

Eccentricity related fault occurs when air gap between the stator and rotor becomes unequal. Air gap eccentricity fault can occur due to inaccurate positioning of the rotor with respect to the stator, bearing wear, stator core movement, shaft deflection, etc. [13]. Two types of eccentricity fault occur in electrical machines. These are dynamic eccentricity (DE) and static eccentricity (SE) faults. These faults are illustrated in Figure 2.

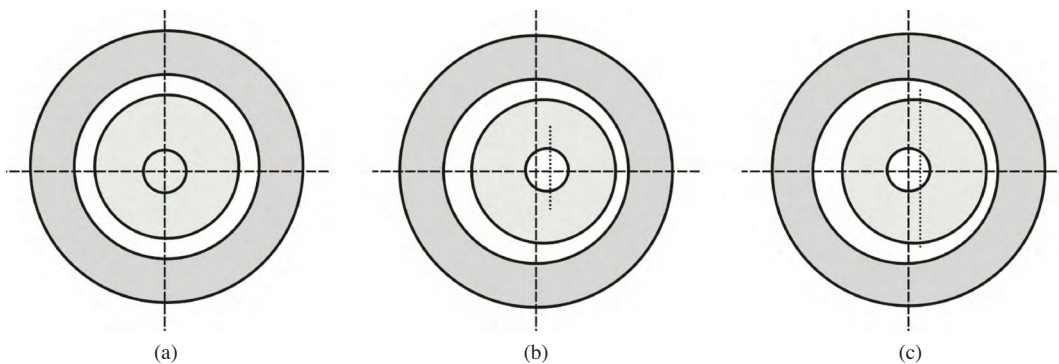


**Figure 2.** Types of eccentricity faults: (a) centric rotor, (b) static eccentricity, and (c) dynamic eccentricity [12].

According to DE, the center of the rotor isn't at the center of the rotation. For this reason the position of minimum air gap rotates with the rotor. Several factors contribute to DE faults, such as a bent rotor shaft, bearing wear or misalignment of bearings, mechanical resonance at critical speed, etc. A SE fault occurs when the rotor rotates about its own centerline, but this centerline does not coincide with that of the stator bore. SE can be caused by oval stator cores or by the incorrect positioning of the stator or rotor [6].

## 2.1. Identification of the static eccentricity

The effects of static eccentricity can be observed via the existence of sideband components that occur around the fundamental frequency in current and voltage spectra. These sideband components are calculated with the equation [1]

$$f_{ecc} = f_s \mp k \cdot f_r. \quad (1)$$

Here,  $f_{ecc}$ ,  $f_s$ ,  $k$  and  $f_r$  are eccentricity frequency, fundamental frequency, an integer and rotational frequency, respectively. In this application these effects are obtained from the spectra while the motor is running at 25% of full load.

## 3. Mathematical methods

In this study, spectral analysis methods are used to detect the static eccentricity of the PMSM. For this purposes, the power spectral density approach and Short-Time Fourier analysis methods are considered as well as coherence approach.

### 3.1. Short-time fourier transform and other spectral analysis methods

The short-time Fourier Transform (STFT) is useful in characterizing the time localization of frequency components of signals. The STFT spectrum is obtained by windowing the signal through a fixed dimension window. The signal may be considered approximately stationary in this window. The window dimension fixes both time and frequency resolutions. To define the STFT, let us consider a signal  $x(t)$  with the assumption that it is stationary when it is windowed through a fixed dimension window  $g(t)$ , centered at time location  $\tau$ . The Fourier transform of the windowed signal yields the STFT [3]

$$STFT(\tau, f) = \int_{-\infty}^{+\infty} x(t) g(t - \tau) \exp[-j2\pi ft] dt. \quad (2)$$

This equation maps the signal into a two-dimensional function in the time-frequency ( $t, f$ ) plane. The analysis depends on the chosen window  $g(t)$ . Once the window  $g(t)$  is chosen, the STFT resolution is fixed over the entire time-frequency plane.

A common approach for extracting the information about the frequency features of a random signal is to transform the signal to the frequency domain by computing the Discrete Fourier Transform (DFT). For a block of data of length  $N$  samples, the transform at frequency  $m\Delta f$  is given by

$$X(m\Delta f) = \sum_{k=0}^{N-1} x(k\Delta t) \exp[-j2\pi km/N], \quad (3)$$

where  $\Delta f$  is the frequency resolution and  $\Delta t$  is the data-sampling interval. The auto-power spectral density (APSD) of  $x(t)$  is estimated as

$$S_{xx}(f) = \frac{1}{N} |X(m\Delta f)|^2, f = m\Delta f. \quad (4)$$

The cross power spectral density (CPSD) between  $x(t)$  and  $y(t)$  is similarly estimated. The statistical accuracy of the estimate in equation (3) increases as the number of data points or the number of blocks of data increases.

The cause and effect relationship between two signals, or the commonality between them, is generally estimated using the coherence function given by

$$\gamma_{xy}(f) = \frac{|S_{xy}(f)|}{\sqrt{S_{xx}(f)S_{yy}(f)}}, 0 < \gamma_{xy} < 1, \quad (5)$$

where  $S_{xx}$  and  $S_{yy}$  are the APSD's of  $x(t)$  and  $y(t)$ , respectively, and  $S_{xy}$  is the CPSD between  $x(t)$  and  $y(t)$ . A value of coherence close to unity indicates highly linear and close relationship between the two signals [17, 18].

## 4. Experimental study and data collection

In this study, the PMSM was used with parameters as given in Table 2. The motor was controlled by using closed loop speed control mode and driven by Pulse Width Modulation (PWM) inverter.

**Table 2.** PMSM nominal data.

Power	0.82 kW
Voltage	$U_{1N} = 147$ V
Pole pairs	$p = 4$
Phases	3
Speed	$n_{max} = 9000$ rpm, $n_n = 3000$ rpm
Torque	$M_0 = 3$ Nm, $M_n = 2.6$ Nm
Current	$I_0 = 3.9$ A, $I_n = 3.5$ A

The purpose of the motor monitoring system is to measure the motor stator current, terminal voltage, motor speed and load torque. The PMSM data was collected at 1 kHz sampling rate at no load condition and 25% load, for healthy and faulty cases. The PMSM drive-fault diagnosis block diagram for the PMSM and motor test bench are shown in Figures 3 and 4 respectively [19].

The block diagram is a typical PMSM drive with speed controller, PWM inverter, speed feedback and current controllers in the dq-axis (rotor rotating reference frame), as shown in Figure 3. Reference speed command is given ( $\omega_r^*$ ) and compared with actual speed  $\omega_r$ . The Proportional-Integral (PI) controller is implemented to operate on the speed error signal. Output of the speed controller is a torque reference command ( $T_q^* = i_q^{r*}$ ); and it is equal to q-axis current command. The reference current is zero for the d-axis ( $i_d^r$ ), because of rotor excitation is produced by permanent magnets. The dq-axis PI current controller outputs produce dq-axis voltage reference command ( $V_d^{r*}, V_q^{r*}$ ). These voltages are applied to PWM inverter to get the voltages that are conveyed to the PMSM stator.

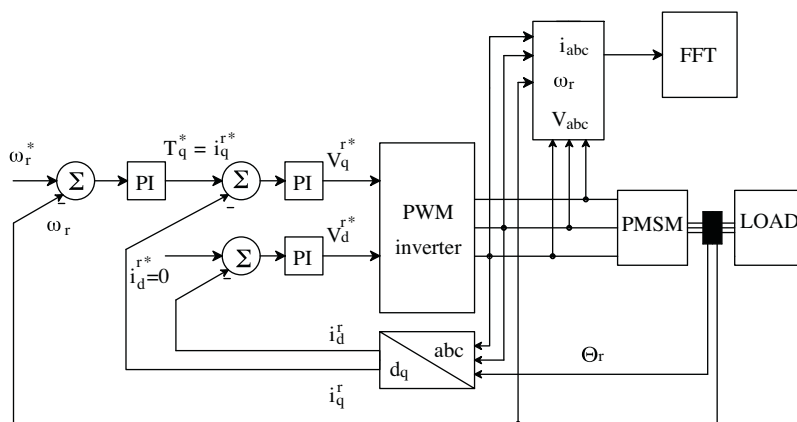


Figure 3. Block diagram for the measurement system.

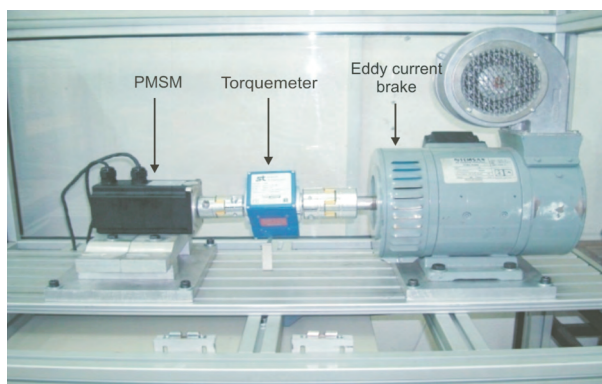


Figure 4. Motor test bench for experimental study.

First, the PMSM was operated at 750 rpm ( $f = 50$  Hz) under no load condition; motor current, voltage, rotor speed and load torque data were collected over the start-up period, up to the 5100 ms. Then SE fault was carried out with a horizontal (angular) misalignment. An angular misalignment was created for PMSM in the horizontal plane, at a specific angle from the original position. Data acquisition process was repeated for the SE fault at motor no-load. Second, the motor was loaded at 25 percent of nominal load for SE fault and signals were acquisitioned over the start-up period, up to 5100 ms. Limitation of the load level is due to the current limitation of the PMSM driver used in this study. Using the experimental study results, time domain variations of the measurements both faulty and healthy cases of the motor are shown in Figure 5.

The different variations are the result of static eccentricity. Also, the time domain analysis results are not informative enough to define the eccentricity characteristics. For this reason, time-frequency domain or frequency domain analysis is needed. These spectral analysis methods are considered in the following section.

## 5. Application for spectral analysis

In this section, the spectral analysis methods are used to define the eccentricity characteristic, for time domain approaches are insufficient here. In this approach, the most effective signal is the motor current signal. In this sense, using the Power Spectral Density (PSD) approach, the spectral properties of the current signal can be compared between the healthy and faulty cases. This situation is shown by Figure 6.

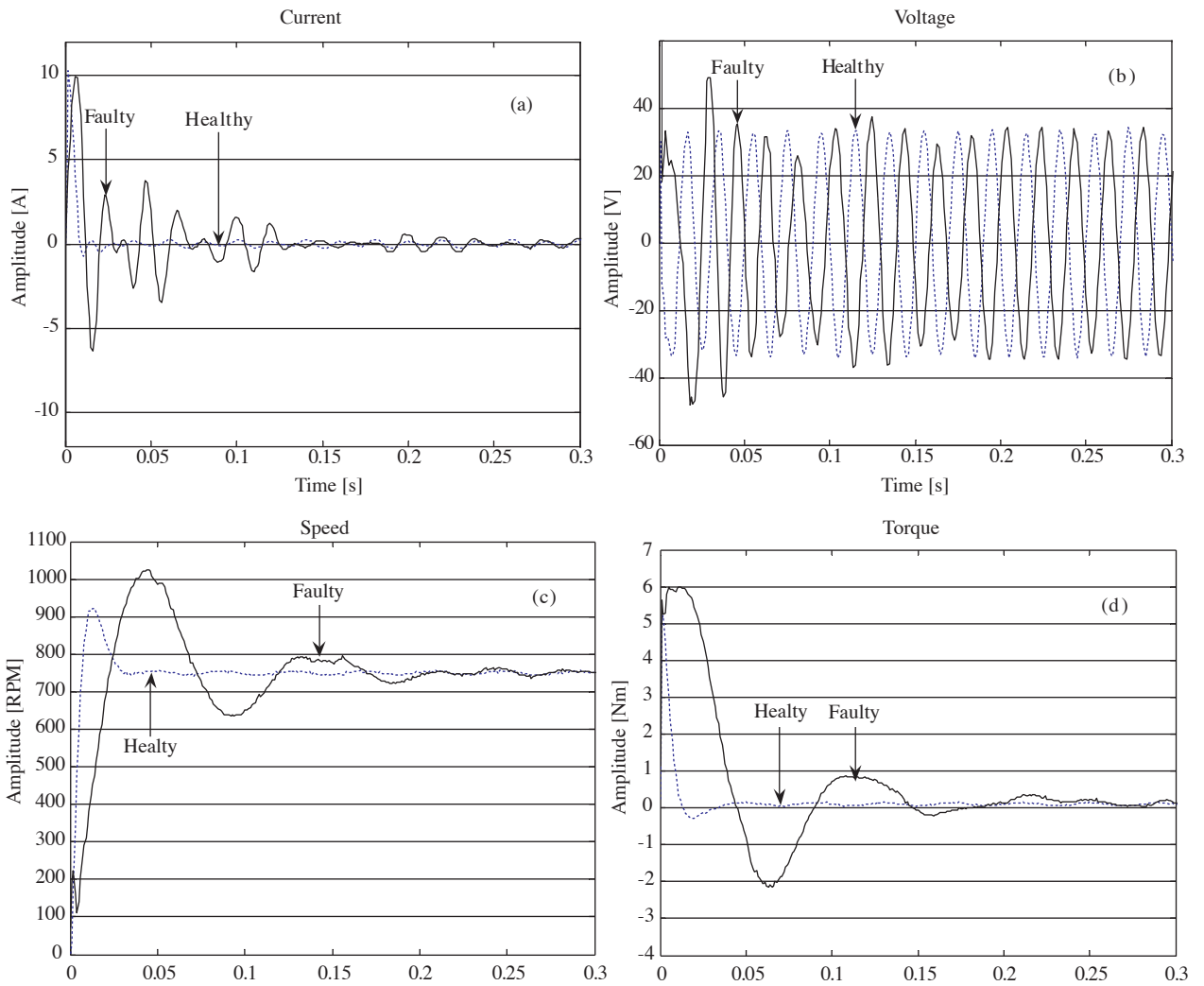


Figure 5. Time-domain comparison of healthy and faulty cases: (a) current, (b) voltage, (c) speed, (d) torque.

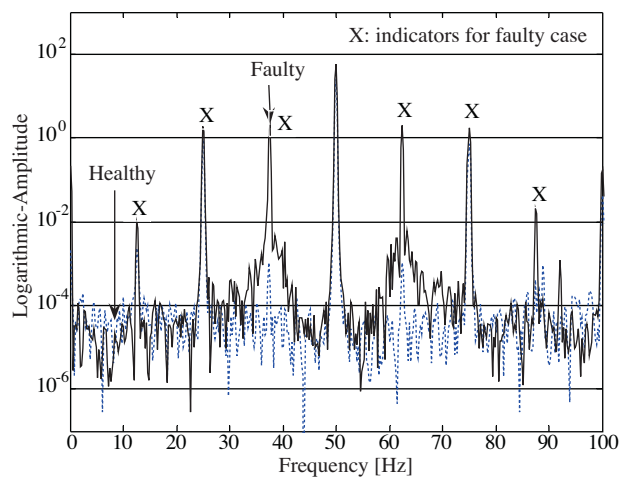
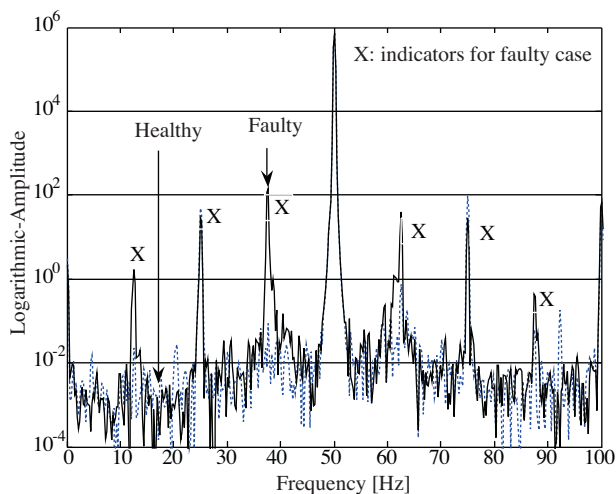


Figure 6. Comparison of current signals for healthy and faulty cases in semi-logarithmic spectral domain.

According to these spectra, which are largely confined between 0 and 100 Hz, the side band amplitudes seen at around the fundamental frequency indicate the eccentricity. The following equalities are used to identify these peak values. Considering the rotational frequency, it is calculated as  $f_r = 750 \text{ rpm}/60 = 12.5 \text{ Hz}$ . Hence, using Equation (1), becomes  $f_{ecc} = 50 \pm k \cdot (12.5)$  for  $k = \pm 1, \pm 2, \pm 3$ , considering the fundamental frequency at 50 Hz. Thus, the eccentricity frequencies are identified by the big amplitudes at 12.5, 25, 37.5, 62.5, 75 and 87.5 Hz. Consequently, the eccentricity is defined with the rotational frequency and its even and odd harmonics depending on the factor  $k$  at around the 50 Hz. Similar results are observed from the voltage spectra in Figure 7.

In terms of the other measurements, such as speed and torque, the effect of the rotational frequency is easily determined from the related figures.

As seen in Figure 8, the amplitudes of the fundamental frequency and the harmonics of the rotational frequency increase as results of the eccentricity. The same characteristic appear for torque variations as seen in Figure 9.



**Figure 7.** Comparison of voltage signals for healthy and faulty cases in semi-logarithmic spectral domain.

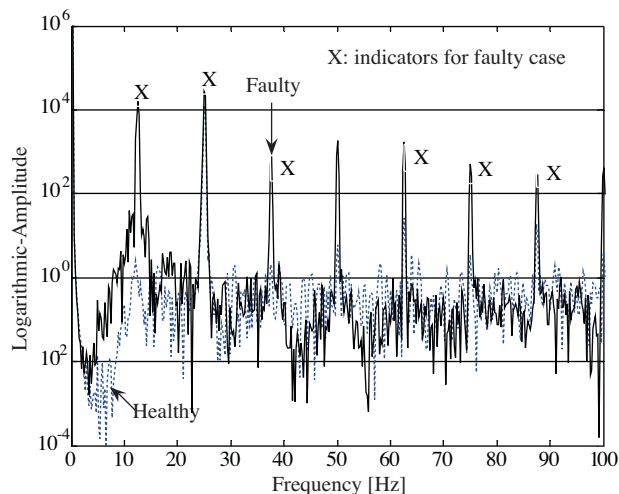


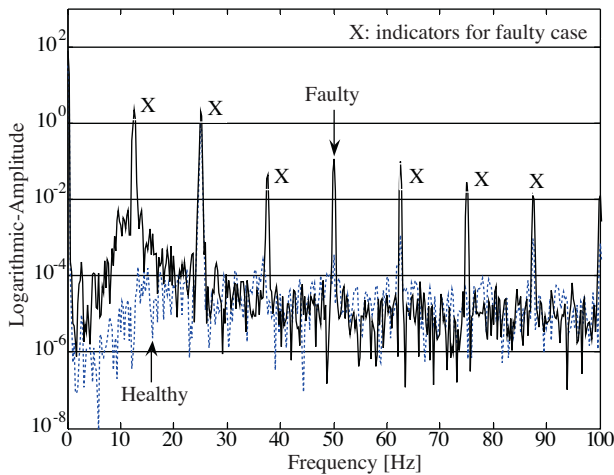
**Figure 8.** Comparison of speed signals for healthy and faulty cases in semi-logarithmic spectral domain.

In Figure 9, the dominant frequency range is determined between 0–150 Hz in terms of the odd and even harmonics of the rotational frequency as well as the fundamental frequency at 50 Hz.

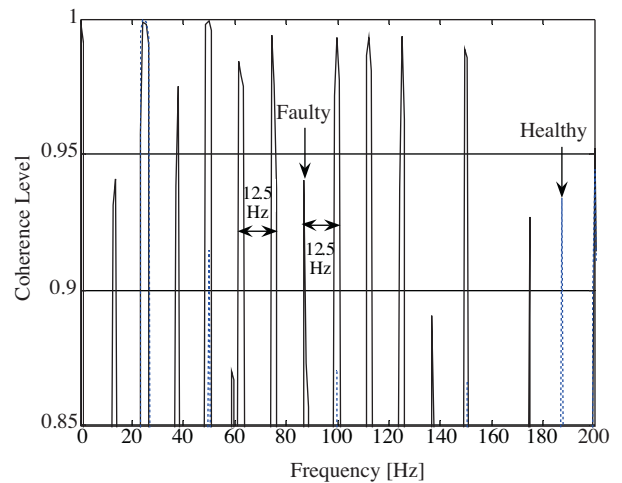
In terms of the coherence analysis, the signal pairs are considered between the motor currents and torque variation. In this manner, using the Equation 5, the related computations are compared between the healthy and faulty cases of the motor.

Figure 10 shows that the highly correlated frequency components between the motor current and torque occur depending on the Equation 1. Hence it can be said that amplitudes of the frequency components like 62.5, 75, and 87.5 Hz etc. increase with the eccentricity. Here, the high coherence levels are evaluated by the threshold at 0.85.





**Figure 9.** Comparison of torque signals for healthy and faulty cases in semi-logarithmic spectral domain.



**Figure 10.** Coherence between current and torque for faulty and healthy cases.

### 5.1. Interpretations on the coherence analysis results

The coherence analysis, which is defined between motor current and torque signals for both of the healthy and faulty cases, can be considered as a contribution to this application in terms of the interpretations on the spectral similarities of the related data. So, in the faulty case, the effect of these similarities is periodically observed at high correlation levels in opposite of the healthy case. This is also described as a feature of the physical process related to the static eccentricity. As a result it can be said that the static eccentricity problem may be revealed by the cross-spectral methods like the coherence approach. Here, the most obvious indicator is the frequency intervals among the highly correlated peaks which is seen as 12.5 Hz. So, this is a feature of the static eccentricity.

## 6. Concluding remarks

This paper reports on a work that investigated the eccentricity problem for PMSM and the analysis was based upon real time measurements. The spectral analysis method, and according to analysis results the eccentricity was defined by the rotational frequency and its harmonics. In detail, the results are:

1. In terms of the electrical quantities such as motor current and voltage variations, the eccentricity is strongly associated with the fundamental frequency and side band effects at around the fundamental.
2. In terms of the mechanical quantities such as motor torque and speed variations, the eccentricity is determined by the rotational frequency and its even and odd harmonics.
3. In terms of the coherence analysis defined between the motor currents and torque variation, for the comparison of the healthy and faulty cases, the eccentricity is determined by the rotational frequencies additional to the fundamental frequency. In this sense, coherence levels at these specific frequencies proportionally increase with the non-uniform magnetic field effect between the rotor and the stator, which indicates the presence of an eccentricity.

Also, these findings are compared with different load condition for 25% of the full load. For this case the current signals in the time domain are shown in Figure 11.

To show the eccentricity for different load conditions, the variations in power spectra for healthy and faulty cases, under no-load condition and under fault at 25% of full load, are compared with one another. From the resulting spectra, together with time-domain observations, the signal power is found to increase with load; and the side band effects found similar to the no-load case.

As seen in Figure 10, for the faulty cases, side bands appeared around the fundamental frequency. However, as indicated in Figure 12, a bias between the no-load and 25% load condition occurs as a result of the change in loads.

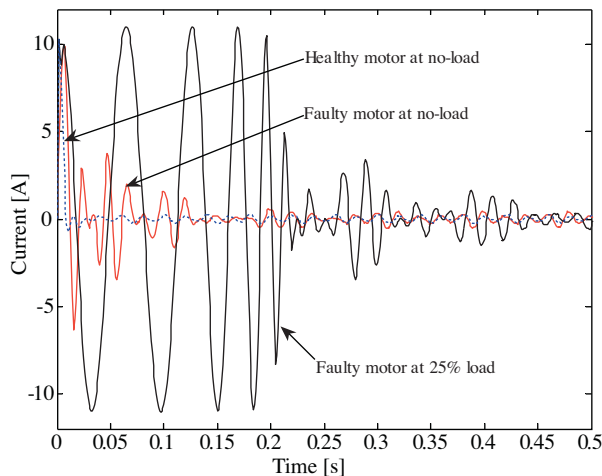


**Figure 11.** Current comparison with different conditions.

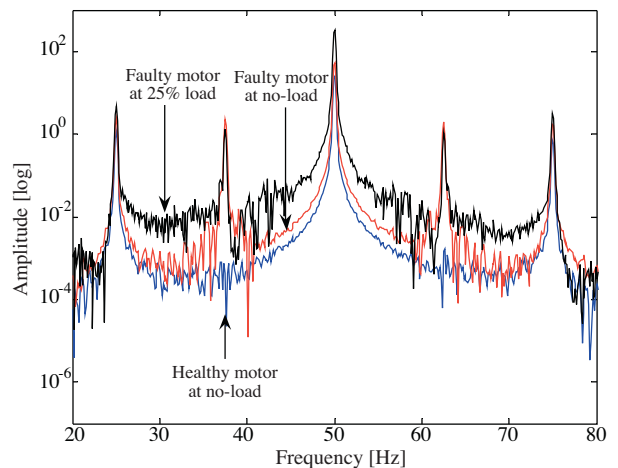


**Figure 12.** Current comparison in frequency domain at different load conditions.

This study presented an original approach to detect the static eccentricity problem using the coherence analysis method as an alternative method to motor current signature analysis. The coherence function based on the normalized cross spectrum technique is defined between the motor current and torque measurements. Hence, the joint properties between the mechanical and electrical quantities are easily revealed as strong relations through this powerful method.

As a future work, in different experimental conditions, it can be repeated using the different mathematical approaches like Wavelet Transform.

## Nomenclature

$x(t)$	Signal
$g(t)$	Fixed dimension window
$\tau$	Centered time location
$\Delta f$	Frequency resolution
$\Delta t$	Data-sampling interval
$\gamma_{xy}$	Coherence function
$S_{xx}$ and $S_{yy}$	Auto-power spectral density of $x(t)$ and $y(t)$
$S_{xy}$	Cross power spectral density between $x(t)$ and $y(t)$

## Abbreviations

STFT Short-Time Fourier Transform  
 APSD Auto-Power Spectral Density  
 CPSD Cross Power Spectral Density

## References

- [1] J. Rosero, J. Cusido, A. Garcia, J. Ortega and L. Romeral, "On-line Condition Monitoring Technique for PMSM Operating with Eccentricity", The 6<sup>th</sup> IEEE International Symposium on Diagnostics for Electric Machines, Power Electronics and Drives, IEEE SDEMPED, Cracow, Poland, pp. 111-116, 2007.
- [2] S. Seker, "Determination of Air-Gap Eccentricity in Electric Motors Using Coherence Analysis", IEEE Power Engineering Review, Vol. 20, No. 7, pp.48-50, 2000.
- [3] S. Seker and E. Ayaz, "A reliability model for induction motor ball bearing degradation", Electric Power Components & Systems, Vol. 31 No. 7, 2003, pp: 639-52, 2003.
- [4] E. Ayaz, S. Seker and A. Ozturk, "Continuous Wavelet Transform for Bearing Damage Detection in Electric Motors", IEEE Melecon, May 16-19, Benalmádena (Málaga), Spain. pp. 1130-33, 2006.
- [5] E. Ayaz, A. Ozturk, S. Seker and B.R. Upadhyaya, "Fault detection based on continuous wavelet transform and sensor fusion in electric motors", Compel, Vol. 28 No.2, pp. 454-70, 2009.
- [6] S. Nandi, H.A. Toliyat and X. Li, "Condition Monitoring and Fault Diagnosis of Electrical Motors - A Review", IEEE Transactions on energy conversion, Vol. 20, No. 4, pp. 719-29, 2005.
- [7] S. Seker and E. Ayaz, "Feature extraction related to bearing damage in electric motors by wavelet analysis", Journal of the Franklin Institute, Vol. 340, No. 2, pp. 125 -34, 2003.
- [8] S. Ozturk, Low-Cost Direct Torque Control of Permanent Magnet Synchronous Motors Using Hall-Effect Sensors, M.S. Thesis, Texas A&M University, College Station, TX, 2005.
- [9] J. Rosero, J. Cusido, A. Garcia, J. Ortega and L. Romeral , "Broken Bearings and Eccentricity Fault Detection for a Permanent Magnet Synchronous Motor" (2006), The 32<sup>nd</sup> Annual Conference of the IEEE Industrial Electronics Society, Paris - France, pp. 964-69, 2006.
- [10] M. B. Ebrahimi, J. Faiz, M. J. Roshtkhari and A. Z. Nejhad, "Static Eccentricity Fault Diagnosis in Permanent Magnet Synchronous Motor Using Time Stepping Finite Element Method", IEEE Transactions on Magnetics, Vol. 44, No. 11, pp. 4297-4300, 2008.
- [11] W. Roux, R. G. Harley and T. G. Habetler, "Detecting Rotor Faults in Low Power Permanent Magnet Synchronous Machines" , IEEE Transactions on Power Electronics, Vol. 22, No. 1, pp. 322-28, 2007.
- [12] M. Akar and I. Cankaya, "Diagnosis of static eccentricity fault in permanent magnet synchronous motor by on-line monitoring of motor current and voltage", Istanbul University-Journal of Electrical and Electronics Engineering (IU-JEEE), Vol. 9, No. 2, pp. 959-967, 2009.

- [13] C. Yeh, A. Sayed and R. Povinelli, "A Reconfigurable Motor for Experimental Emulation of Stator Winding Inter-Turn and Broken Bar Faults in Polyphase Induction Machines", *IEEE Transactions on Energy Conversion*, Vol. 23, No. 4, pp. 1005-14, 2008.
- [14] C. Kral, T.G. Habetler and R.G. Harley, "Detection of Mechanical Imbalances of Induction Machines Without Spectral Analysis of Time-Domain Signals", *IEEE Transactions on Industry Applications*, Vol. 40, No. 4, pp. 1101-06, 2004.
- [15] P. Vas, *Parameter Estimation, Condition Monitoring, and Diagnosis of Electrical Machines*, Clarendon Press, Oxford, 1993.
- [16] S. Rajagopalan, *Detection of Rotor and Load Faults in Brushless DC Motors Operating under stationary and un-stationary conditions*, PhD Thesis, School of Electrical and Computer Engineering, Georgia Institute of Technology, 2006.
- [17] S. Taskin, S. Seker, M. Karahan and C. Akinci, "Spectral analysis for current and temperature measurements in power cables", *Electric Power Components & Systems*, Vol. 37, No. 4, pp. 415-26, 2009.
- [18] S. V. Vaseghi, *Advanced Signal Processing and Digital Noise Reduction*, John Wiley & Sons Inc., Chichester, England, 1996.
- [19] M. Akar, "Mechanical fault diagnosis in the permanent magnet synchronous motor with artificial intelligence techniques"(in Turkish), PhD Thesis, University of Sakarya, pp.66, 2009.